DOI: 10.1002/ejic.201100052

Versatile Coordination Modes of 2-(Diformylmethylene)-3,3-dimethylindole towards Late-Transition-Metal Ions: C–H Bond Activation and Formation of Cyclic Acyl–Palladium(II) Complexes

Hamid Khaledi,*[a] Hapipah Mohd Ali,[a] and Marilyn M. Olmstead[b]

Keywords: Ligand design / Transition metals / Coordination modes / C–H activation / Anagostic interactions

The reaction of the potential multidentate ligand, 2-(diformylmethylene)-3,3-dimethylindole (diformyl), with $M(OAc)_2$ (M = Co^{II}, Ni^{II}, Cu^{II}, Zn^{II}, Cd^{II}, and Pd^{II}) afforded a series of metal complexes with different nuclearity in which the mono-deprotonated diformyl behaves as an *N*,*O*-bidentate chelate or *N*,*O*,*O*-tridentate chelating-bridging agent. The bonding modes of the ligand and thus the structures could be modified to some extent by further treatment of the complexes with an ancillary ligand (methanol, pyridine, or 4,4′-bipyridine). In the case of the palladium(II) complex, the pyridine and 4,4′-bipyridine adducts yielded *C*,*N*-chelation of the metal ion through the aldehyde carbon and indolic nitrogen of the doubly deprotonated diformyl. The resulting acyl–palladium complexes were further bridged into polymeric structures when the dianionic diformyl behaved as a *C*,*N*,*O*-chelating-bridging ligand.

Introduction

The combination of coordinate bonding with intermolecular interactions, such as hydrogen bonding and π–π interactions, in metal complexes of multidentate organic ligands provides intriguing prospects for the design of novel metal-organic supramolecular architectures. In this context, the geometries of the metal centers and certain features of the ligands, such as flexibility, versatile bonding modes, and the ability to undertake hydrogen bonding, can heavily control the self-assembly process, and thus the structure and properties of the products. The architecture of the products can be predictable to a high degree when rigid ligands are used,[1–3] whereas utilizing ligands with more flexibility reduces the structure predetermination and may afford unique frameworks with interesting properties.[4–6]

Some years ago, Helliwell and co-workers described the synthesis and crystal structure of 2-(diformylmethylene)-3,3-dimethylindole.[7] We have recently reported the structure of a second polymorph of this compound that differs from the former by a 180° rotation of one formyl group.[8] The structure of this aminomethylene-malonaldehyde offers an interesting potential ambidentate ligand on account of the presence of disparate coordination sites capable of showing ketoamine–enolimine tautomerism (Figure 1).

Figure 1. Tautomeric forms of 2-(diformylmethylene)-3,3-dimethylindole.

We now report the results of our studies on coordination behavior of 2-(diformylmethylene)-3,3-dimethylindole (diformyl) towards Co^{II}, Ni^{II}, Cu^{II}, Zn^{II}, Cd^{II}, and Pd^{II} ions. To gain a deeper insight into the coordination chemistry of the ligand, where possible the initial complexes were further modified by ancillary ligands.

Results and Discussion

2-(Diformylmethylene)-3,3-dimethylindole is the diformylation product of the reaction of 2,3,3-trimethylindolenine with Vilsmeier reagent ($DMF/POCl_3$). The compound may, in principle, exist in the two tautomeric forms depicted in Figure 1. In the solid state, as revealed by X-ray crystallography, the compound presents the ketoamine form.[7,8] The NMR spectroscopic data suggest that also in $CDCl_3$ the ketoamine tautomer is preferred over the enolimine form. The ^1H NMR spectrum shows the two formyl protons at δ = 9.79 and 9.77 ppm and the N*H* signal at δ = 13.56 ppm, whereas the ^{13}C NMR spectroscopic signals of the formyl carbon atoms appear at δ = 192.43 and 187.85 ppm. These values are indicative of the ketoamine

[a] Department of Chemistry, University of Malaya, 50603 Kuala Lumpur, Malaysia
Fax: +603-79674193
E-mail: khaledi@siswa.um.edu.my
hamid.khaledi@gmail.com
[b] Department of Chemistry, University of California, One Shields Avenue, Davis, CA 95616, USA

form as discussed earlier by Neuvonen et al.[9] Upon the reaction with $M(OAc)_2$ (M = Co^{II}, Ni^{II}, Cu^{II}, Zn^{II}, Cd^{II}, or Pd^{II}) in ethanol and in the presence of triethylamine, the diformyl compound loses its amino proton to ligate the metal ions as a monoanionic ligand. This is reflected in omission of the υ(N–H) band of the ligand at 3146 cm^{-1} in the IR spectra of the obtained metal complexes. The elemental analyses for complexes of Cu^{II} (**5**), Zn^{II} (**6**), Cd^{II} (**8**), and Pd^{II} (**10**) ions are consistent with the formula $[M(C_{13}H_{12}NO_2)_2]$, whereas for the Co^{II} (**1**) and Ni^{II} (**3**) complexes they suggest the presence of one and two molecules of water. The magnetic susceptibility value of $[Co(C_{13}H_{12}NO_2)_2(H_2O)]$ (**1**) (5.41 B.M.) indicates a high-spin configuration with significant orbital contribution, characteristic of an octahedral Co^{II} complex. Similarly, the magnetic moment of $[Ni(C_{13}H_{12}NO_2)_2(H_2O)_2]$ (**3**) (2.97 B.M.) is typical of a high-spin octahedral nickel(II) complex. Regrettably, no suitable single crystals could be obtained from these two compounds; however, on treatment with pyridine (py), $[Co(C_{13}H_{12}NO_2)_2(py)_2]$ (**2**) and $[Ni(C_{13}H_{12}NO_2)_2(py)_2]$ (**4**) were obtained as proper crystals for X-ray analysis. Our attempt to treat the Cu^{II} (**5**), Zn^{II} (**6**), and Cd^{II} (**8**) complexes with pyridine were unsuccessful; nevertheless, the zinc and cadmium complexes reacted with methanol to give the corresponding methanol adducts with the formula $[M(C_{13}H_{12}NO_2)_2(MeOH)_2]$ (**7** and **9**). The IR spectra of **7** and **9** show the υ(O–H) as broad bands (2700–3400 cm^{-1}) and the υ(C–O) of the methanol moieties at 1034 and 1033 cm^{-1}. The palladium(II) complex **10** is diamagnetic and soluble in chloroform. The ^1H NMR spectrum of **10**, when compared to that of diformyl, shows a significant upfield shift ($\delta \approx 2$ ppm) of one of the C*H*O signals upon complexation, whereas the position of the other C*H*O is little altered. Moreover the N*H* resonance of the ligand is absent in the spectrum of the palladium complex. Compound **10** reacted with pyridine in DMF to give the crystalline compounds of **11** and **12**. In a similar way, treatment of **10** with 4,4′-bipyridine in DMF led to the formation of **13**.

Except for compounds **1** and **3**, the three-dimensional structures of the complexes were fully determined by X-ray crystallographic analysis.

Crystal Structures of Cobalt(II) and Nickel(II) Complexes (2 and 4)

Recrystallization of **1** and **3** in the presence of pyridine afforded the crystals of **2** and **4** (Scheme 1), respectively, the structures of which are isomorphous and consist of discrete mononuclear molecules.

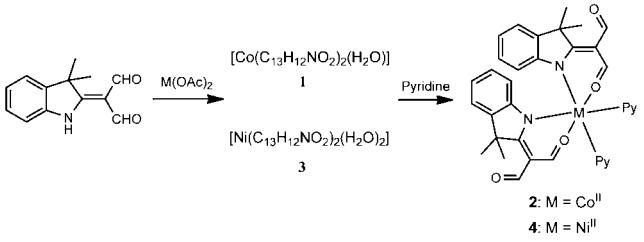

Scheme 1.

The structure of the Co complex **2** is shown in Figure 2. In the molecules, the deprotonated diformyl ligands act as *N*,*O*-bidentate chelates to form six-membered rings with the metal centers. Whereas one of the carbonyl oxygen atoms of the diformyl ligand is involved in the coordination, the

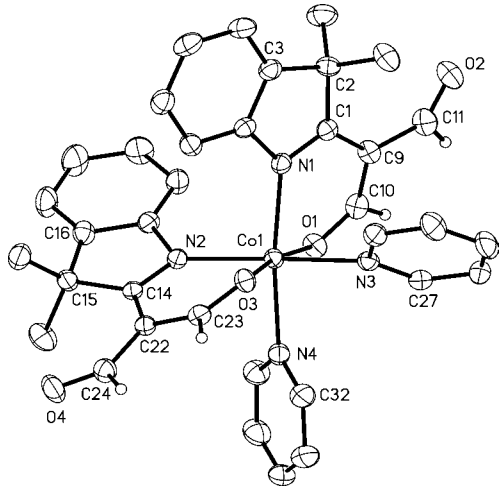

Figure 2. The molecular structures and labeling schemes of complex **2** (50% probability ellipsoids). Hydrogen atoms, except for the aldehyde hydrogen atoms, have been omitted for clarity.

Table 1. Hydrogen-bond geometry for **2**, **4**, and **5**.[a]

D–H···A	H···A [Å]	D···A [Å]	D–H···A [°]
$[Co(C_{13}H_{12}NO_2)_2(py)_2]$ (**2**)			
C4–H4···O4#1	2.49	3.425(4)	167.8
C12–H12B···O2	2.24	3.039(4)	138.0
C13–H13B···O2	2.34	3.114(4)	134.9
C20–H20···O1	2.58	3.291(3)	132.2
C25–H25B···O4	2.21	3.017(4)	138.7
C26–H26B···O4	2.43	3.184(4)	133.1
C28–H28···O4#2	2.46	3.168(4)	131.5
C31–H31···O3	2.48	2.955(3)	110.7
C34–H34···O2#3	2.56	3.225(4)	127.5
$[Ni(C_{13}H_{12}NO_2)_2(py)_2]$ (**4**)			
C4–H4···O4#2	2.57	3.472(6)	162.6
C7–H7···O3	2.58	3.169(5)	121.8
C12–H12B···O2	2.28	3.059(6)	138.3
C13–H13B···O2	2.42	3.160(7)	133.7
C20–H20···O1	2.56	3.196(5)	125.9
C25–H25B···O4	2.20	2.999(6)	140.4
C26–H26B···O4	2.53	3.249(5)	131.8
C29–H29···O4#1	2.53	3.158(6)	125.3
C31–H31···O3	2.44	2.905(5)	111.2
C34–H34···O2#4	2.49	3.213(7)	135.1
$[Cu(C_{13}H_{12}NO_2)_2]_2$ (**5**)			
C7–H7···O3	2.37	2.925(5)	116.6
C12–H12B···O2	2.26	3.056(6)	137.5
C13–H13B···O2	2.32	3.090(6)	135.0
C20–H20···O1	2.52	3.009(5)	111.9
C25–H25B···O4	2.56	3.291(6)	131.8
C26–H26B···O4	2.25	3.053(6)	138.5

[a] Symmetry transformations used to generate equivalent atoms: #1 x, $y-1$, z; #2 $x+1$,$y-1$, z; #3 x, $y+1$, z; #4 $x-1$,$y+1$, z.

Table 2. Selected bond lengths [Å] and bond angles [°] for **2**, **4**, and **5**.[a]

$[Co(C_{13}H_{12}NO_2)_2(py)_2]$ (**2**)		$[Ni(C_{13}H_{12}NO_2)_2(py)_2]$ (**4**)		$[Cu(C_{13}H_{12}NO_2)_2]_2$ (**5**)	
Bond lengths					
M–O1	2.0322(18)	M–O1	2.001(3)	M–O1	1.923(3)
M–O3	2.0278(18)	M–O3	2.019(3)	M–O3	1.937(3)
M–N1	2.110(2)	M–N1	2.073(3)	M–N1	1.952(4)
M–N2	2.115(2)	M–N2	2.077(3)	M–N2	1.954(3)
M–N3	2.214(2)	M–N3	2.148(3)	M–O4#1	2.580(3)
M–N4	2.180(2)	M–N4	2.144(3)		
Bond angles					
O3–M–O1	170.58(8)	O3–M–O1	172.72(11)	O1–M–O3	167.62(13)
O3–M–N1	100.32(8)	O3–M–N2	86.21(12)	O1–M–N1	90.78(13)
O1–M–N1	84.88(8)	O1–M–N2	98.17(12)	O3–M–N1	93.27(13)
O3–M–N2	85.56(8)	O3–M–N1	98.88(11)	O1–M–N2	90.12(13)
O1–M–N2	101.84(8)	O1–M–N1	86.59(12)	O3–M–N2	88.89(13)
N1–M–N2	95.60(8)	N2–M–N1	95.01(12)	N1–M–N2	165.41(14)
O3–M–N4	89.54(8)	O3–M–N3	84.50(12)	O1–M–O4#1	85.19(12)
O1–M–N4	84.77(8)	O1–M–N3	91.07(13)	O3–M–O4#1	82.90(12)
N1–M–N4	169.25(8)	N2–M–N3	170.70(13)	N1–M–O4#1	93.31(13)
N2–M–N4	89.39(8)	N1–M–N3	86.57(12)	N2–M–O4#1	101.27(12)
O3–M–N3	83.00(8)	O3–M–N4	89.24(12)		
O1–M–N3	89.64(8)	O1–M–N4	84.99(13)		
N1–M–N3	85.42(8)	N2–M–N4	89.51(12)		
N2–M–N3	168.51(8)	N1–M–N4	170.93(13)		
N4–M–N3	91.59(8)	N3–M–N4	90.23(13)		

[a] Symmetry transformations used to generate equivalent atoms: #1 $-x+1, -y+1, -z+2$.

other one remains uncoordinated and engaged in intra- and intermolecular C–H···O hydrogen-bonding interactions (Table 1). The Co^{II} and Ni^{II} ions are six-coordinate by two diformyl ligands and two *cis*-located pyridine molecules in a distorted octahedral geometry.

The $Co–N_{py}$ bond lengths, 2.214(2) and 2.180(2) Å, are somewhat longer than those observed in similar coordination systems,[10,11] whereas the $Ni–N_{py}$ bond lengths, 2.144(3) and 2.148(3) Å, are in agreement with the values reported in the literature.[12,13] Selected values of bond lengths and bond angles for **2** and **4** are shown in Table 2.

Crystal Structure of Copper(II) Complex 5

In the copper(II) complex **5**, the deprotonated diformyl ligand behaves in two fashions (i.e., *N*,*O*-bidentate chelating and *N*,*O*,*O*-tridentate chelating bridging), which leads to discrete dinuclear complexes (Scheme 2).

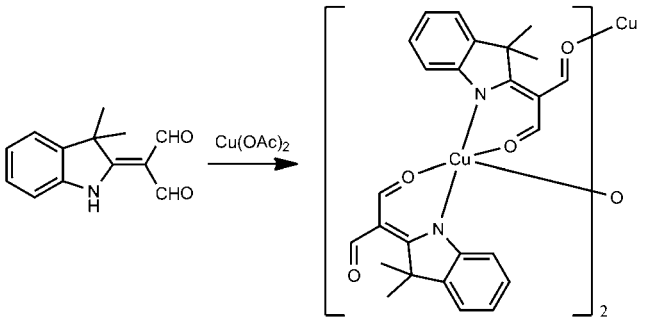

Scheme 2.

The crystal structure of **5** is shown in Figure 3. In the molecule, the copper atom adopts a slightly distorted square-pyramidal coordination geometry with τ value[14] of 0.04. The basal plane is defined by two nitrogen and two oxygen atoms afforded by two diformyl ligands, and the apical position is occupied by the O4 atom from a symmetry-related ligand with Cu–O4 distance of 2.580(4) Å. Within the resulting centrosymmetric dimer, the copper atoms are separated by 6.9404(14) Å. The uncoordinated carbonyl oxygen atom (O2) is involved in C–H···O hydrogen-bonding interactions (Table 1).

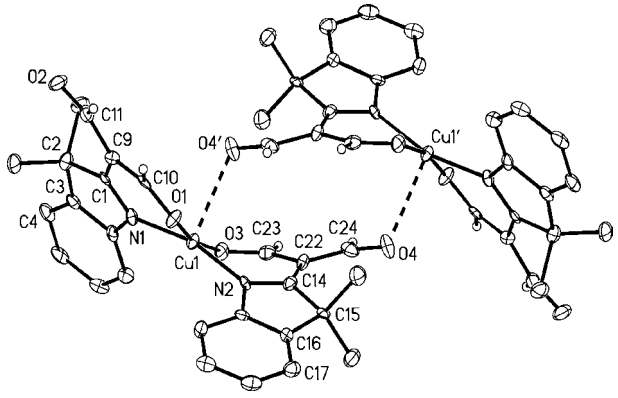

Figure 3. A perspective view of the dimeric structure of complex **5** (50% probability ellipsoids). The hydrogen atoms, except for the aldehyde hydrogen atoms, have been omitted for clarity.

Selected geometrical parameters for the copper(II) complex are listed in Table 2. The Cu–O and Cu–N bond lengths are comparable to those in $[Cu_2\{(3,5\text{-}NO_2)_2sal\}_2$-

$(2,2'\text{-bipy})_2]\cdot 0.5H_2O$, a dinuclear copper(II) complex with a similar coordination environment.[15]

Crystal Structures of Zinc(II) and Cadmium(II) Complexes

The anionic diformyl ligand showed the same behavior toward Zn^{II} and Cd^{II} ions. It formed isostructural complexes $[Zn(C_{13}H_{12}NO_2)_2]$ (**6**) and $[Cd(C_{13}H_{12}NO_2)_2]$ (**8**). In these complexes, as shown in Figure 4 (a) for the Zn complex, the ligand employs all three nitrogen and oxygen atoms in a chelating-bridging coordination fashion. The metal atoms, placed on inversion centers, are octahedrally coordinated by two nitrogen and two oxygen (O1) atoms provided by two diformyl chelates in the equatorial plane and two axially positioned oxygen (O2) atoms from two symmetry-related ligands. The overall result is three-dimensional polymeric structures with cylindrical channels in the [111] direction (Figure 4, b). The total potential void volume of the unit cell is 219.4 Å^3 (12.3% of the cell volume) in the zinc complex and 263.5 Å^3 (13.9% of the cell volume) in the cadmium complex, as estimated by PLATON software.[16]

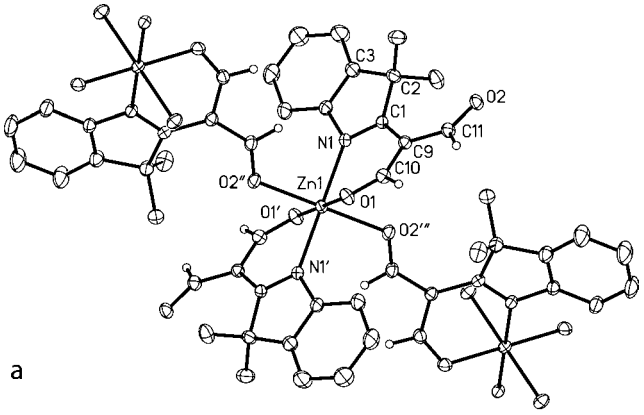

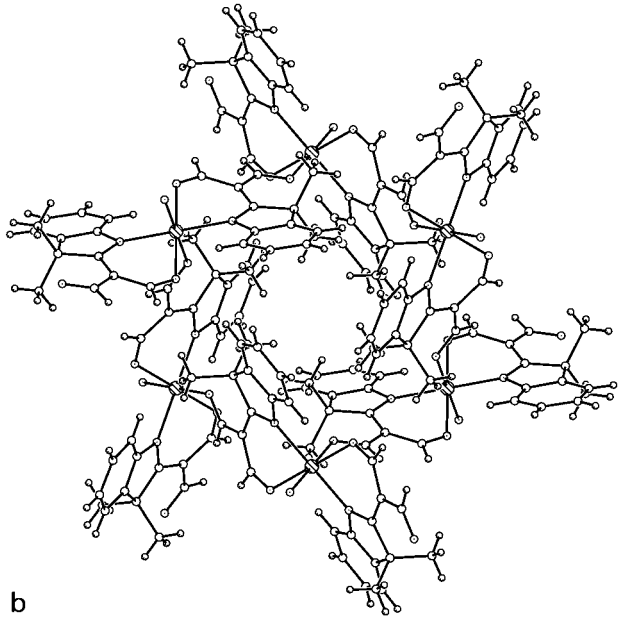

Figure 4. (a) The molecular structure of complex **6** (30% probability ellipsoids). The hydrogen atoms, except for the aldehyde hydrogen atoms, have been omitted for clarity. (b) Packing view of **6** showing a cylindrical channel.

The coordination geometry of the zinc complex deviates slightly from an ideal octahedron as reflected by the *cisoid* angles of 83.36(5)–96.64(5)°. Similarly, but to a larger extent, the cadmium complex shows a distortion, the *cisoid* angles being 78.47(5)–101.53(5)°. Selected bond lengths and bond angles for the complexes **6** and **8** are listed in Table 3.

Coordination polymers **6** and **8** did not react with pyridine, however upon treatment with methanol, their three-dimensional networks were cleaved to form discrete mononuclear methanol adducts, **7** and **9** (Scheme 3).

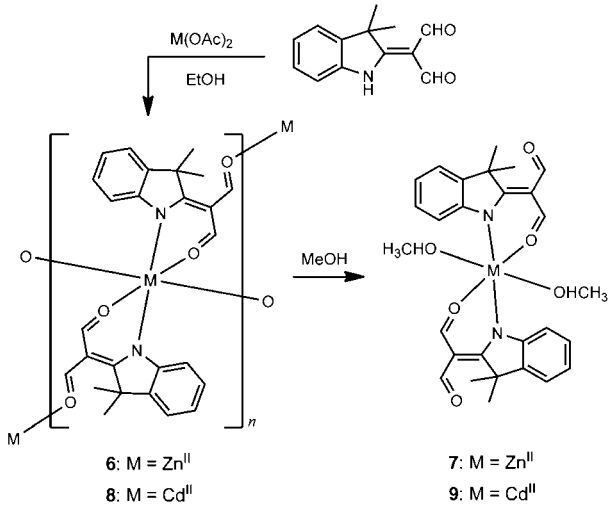

Scheme 3.

These two complexes are isostructural, wherein the anionic diformyl ligand acts as an *N*,*O*-bidentate chelate. The structure of the Zn complex is shown in Figure 5. The metal atom is located on a center of inversion and coordinated by two diformyl chelates and two *trans*-located methanol molecules in a distorted octahedral geometry. The uncoordinated formyl oxygen atoms are hydrogen bonded to the methanol hydroxy groups of the adjacent molecules (Table 4), which results in infinite hydrogen-bonded chains along the crystallographic *b* axis.

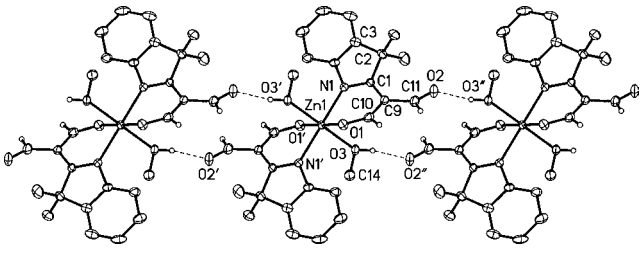

Figure 5. The crystal structure of complex **7** showing the atom-labeling scheme and the O–H···O intermolecular hydrogen bonding (50% probability ellipsoids). The hydrogen atoms, except for the hydroxy and aldehyde hydrogen atoms, have been omitted for clarity.

Table 3. Selected bond lengths [Å] and bond angles [°] for **6**, **7**, **8**, and **9**.[a]

$[Zn(C_{13}H_{12}NO_2)_2]_n$ (**6**)		$[Zn(C_{13}H_{12}NO_2)_2(CH_4O)_2]$ (**7**)		$[Cd(C_{13}H_{12}NO_2)_2]_n$ (**8**)		$[Cd(C_{13}H_{12}NO_2)_2(CH_4O)_2]$ (**9**)	
Bond lengths							
M–N1	2.1053(13)	M–N1	2.1060(15)	M–N1	2.2693(14)	M–N1	2.2590(13)
M–O1	2.0719(12)	M–O1	2.0804(14)	M–O1	2.2733(12)	M–O1	2.2826(11)
M–O2#1	2.2226(11)	M–O3	2.1968(13)	M–O2#1	2.3344(12)	M–O3	2.3502(11)
Bond angles							
N1–M–N1#2	180.0	N1–M–N1#4	180.0	N1–M–N1#2	180.0	N1–M–N1#4	180.0
N1–M–O1	83.36(5)	N1–M–O1	84.60(5)	N1–M–O1	78.47(5)	N1–M–O1	79.14(4)
O1–M–O1#2	180.0	O1–M–O1#4	180.0	O1–M–O1#2	180.0	O1–M–O1#4	180.0
O1–M–O2#1	90.25(5)	O1–M–O3	92.22(6)	O1–M–O2#1	90.84(4)	O1–M–O3	90.66(4)
N1–M–O2#1	91.24(5)	N1–M–O3	89.35(6)	N1–M–O2#1	91.32(5)	N1–M–O3	89.63(4)
O2#1–M–O2#3	180.0	O3–M–O3#4	180.0	O2#1–M–O2#3	180.0	O3–M–O3#4	180.0

[a] Symmetry transformations used to generate equivalent atoms: #1 x, $y + 1$, z; #2 $-x + 1$, $-y + 1$, $-z + 2$; #3 $-x + 1$, $-y + 1$, $-z + 1$; #4 $-x + 2$, $-y$, $-z$.

Table 4. Hydrogen-bond geometry for **7** and **9**.[a]

D–H···A	H···A [Å]	D···A [Å]	D–H···A [°]
$[Zn(C_{13}H_{12}NO_2)_2(CH_4O)_2]$ (**7**)			
O3–H3···O2#1	2.52	3.182(3)	127.0
C11–H11···O1#2	2.58	3.506(3)	165.1
C12–H12B···O2	2.23	3.027(3)	137.8
C13–H13B···O2	2.51	3.233(3)	130.6
C7–H7···O1#3	2.52	3.182(3)	127.0
$[Cd(C_{13}H_{12}NO_2)_2(CH_4O)_2]$ (**9**)			
O3–H3···O2#1	1.826(16)	2.6214(18)	168(2)
C11–H11···O1#2	2.57	3.497(2)	165.8
C12–H12B···O2	2.20	3.002(2)	138.2
C13–H13B···O2	2.53	3.249(2)	130.5

[a] Symmetry transformations used to generate equivalent atoms: #1 $-x + 2$, $-y + 1$, $-z$; #2 $-x + 2$, $y + ½$, $-z - ½$; #3 $-x + 2$, $-y$, $-z$.

Table 3 summarizes the bond lengths and angles for the zinc(II) and cadmium(II) complexes. The Zn–O and Zn–N bond lengths are in agreement with the values reported for similar coordination systems[17,18] as are the Cd–O and Cd–N bond lengths.[19]

Crystal Structures of Palladium(II) Complexes 10, 11, 12, and 13

The crystal of **10** suitable for X-ray analysis was obtained from a dioxane solution at room temperature. As depicted in Figure 6, the monoanionic diformyl ligand acts as an *N*,*O*-bidentate chelate to form six-membered rings with the metal center in a distorted square-planar coordination environment.

The distortion is evident from the deviation (0.044 Å) of the palladium atom from the coordination plane (N1, N2, O1, O3) and also the N1–Pd1–N2 and O1–Pd1–O3 bond angles of 176.7(3)° and 171.6(3)° (Table 5). Six-membered palladium(II) metallocycles with an $N,O_{aldehyde}$-bidentate chelate are unprecedented; however, those with N,O_{ketone} ligands have been reported and have similar Pd–N and Pd–O bond lengths to those of the present structure.[20–22] The Pd cation is also involved in a long-range interaction with the apically placed O4 atom of a symmetry-related molecule with Pd···O distance of 3.141(8) Å, which leads to a dimeric, pseudo-square-pyramidal geometry around the palladium atom. This arrangement is similar to what was observed in dimeric copper(II) complex **5**; however, the Pd···O4 distance is much longer than those usually considered as bonding interactions (ca. 2.06 Å) and can only be indicative of a weak interaction. A similar interaction has been reported for a few palladium complexes with the Pd···O distances ranging between 2.734–3.303 Å.[23–25] The uncoordinated carbonyl oxygen atom O2 is engaged in intra- and intermolecular C–H···O hydrogen bonding (Table 6).

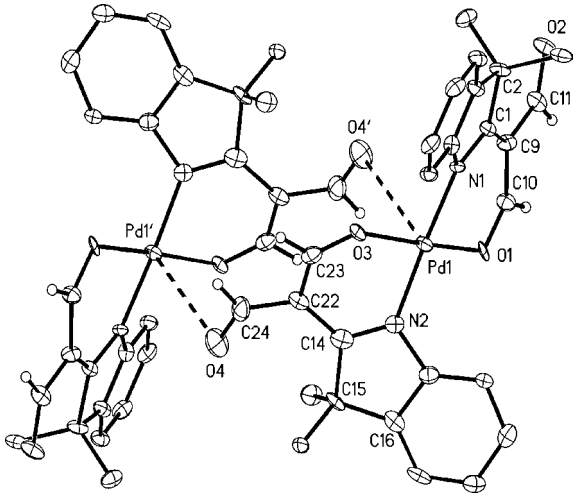

Figure 6. A perspective view of two molecules of **10** showing dimerization through Pd1···O4 interactions. Displacement ellipsoids are drawn at the 50% probability level. The hydrogen atoms, except for the aldehyde hydrogen atoms, have been omitted for clarity.

Treatment of the palladium(II) complex **10** with pyridine in DMF afforded concomitant crystallization of two different pyridine coordinated complexes, **11** and **12** (Scheme 4).

Table 5. Selected bond lengths [Å] and bond angles [°] for **10**, **11**, **12**, and **13**.[a]

$[Pd(C_{13}H_{12}NO_2)_2]$ (**10**)		$[Pd(C_{13}H_{11}NO_2)(py)]_n$ (**11**)		$[Pd(C_{13}H_{11}NO_2)(py)_2]$ (**12**)		$\{[Pd(C_{13}H_{11}NO_2)(bipy)]\cdot 0.5DMF\}_n$ (**13**)	
Bond lengths							
M–O1	1.998(6)	M–C10	1.971(2)	M–C10	1.997(3)	M–C10	1.993(2)
M–N1	2.002(8)	M–N1	2.0322(17)	M–N1	2.032(2)	M–N1	2.0278(18)
M–N2	2.002(8)	M–N2	2.0765(18)	M–N2	2.079(3)	M–N2	2.0955(19)
M–O3	2.016(7)	M–O2#1	2.2355(14)	M–N3	2.232(3)	M–N3	2.2205(19)
Bond angles							
O1–M–N1	90.7(3)	C10–M–N1	80.95(8)	C10–M–N1	80.88(12)	C10–M–N1	80.95(8)
O1–M–N2	88.9(3)	C10–M–N2	93.72(8)	C10–M–N2	91.51(12)	C10–M–N2	93.75(9)
N1–M–N2	176.7(3)	N1–M–N2	174.52(6)	N1–M–N2	172.02(10)	N1–M–N2	174.36(7)
O1–M–O3	171.6(3)	C10–M–O2#1	176.96(7)	C10–M–N3	177.16(11)	C10–M–N3	178.88(8)
N1–M–O3	90.8(3)	N1–M–O2#1	99.65(6)	N1–M–N3	101.57(10)	N1–M–N3	99.95(7)
N2–M–O3	90.0(3)	N2–M–O2#1	85.61(6)	N2–M–N3	86.10(10)	N2–M–N3	85.38(7)

[a] Symmetry transformations used to generate equivalent atoms: #1 $x, -y + ½, z + ½$.

Table 6. Hydrogen-bond geometry for **10**, **11**, and **12**.[a]

D–H···A	H···A [Å]	D···A [Å]	D–H···A [°]
$[Pd(C_{13}H_{12}NO_2)_2]$ (**10**)			
C5–H5···O2#1	2.56	3.487(12)	164.3
C7–H7···O3	2.31	2.888(12)	118.3
C12–H12B···O2	2.28	3.063(12)	136.3
C13–H13B···O2	2.26	3.047(13)	136.5
C20–H20···O1	2.37	2.899(11)	114.9
C25–H25B···O4	2.35	3.107(13)	133.8
C26–H26B···O4	2.28	3.065(14)	136.6
$[Pd(C_{13}H_{11}NO_2)(py)]_n$ (**11**)			
C6–H6···O1#2	2.45	3.370(3)	162.1
C7–H7···O2#3	2.48	3.265(3)	139.7
C11–H11···O1	2.41	2.788(3)	103.7
C12–H12B···O2	2.36	3.152(2)	137.6
C12–H12C···O1#4	2.45	3.394(3)	161.8
C15–H15···O1#5	2.45	3.175(3)	133.3
C18–H18···O1	2.44	2.824(3)	104.0
$[Pd(C_{13}H_{11}NO_2)(py)_2]$ (**12**)			
C4–H4···O1#6	2.57	3.480(4)	166.1
C11–H11···O1	2.50	2.852(5)	102.3
C12–H12C···O2	2.47	3.216(6)	134.7
C13–H13A···O2	2.40	3.176(6)	137.4
C21–H21···O2#7	2.56	3.223(6)	129.0
C23–H23···O1#8	2.50	3.418(5)	169.5

[a] Symmetry transformations used to generate equivalent atoms: #1 $x - 1, -y + {}^3/_2, z + ½$; #2 $x - 1, -y + ½, z + ½$; #3 $x, -y + ½, z + ½$; #4 $x - 1, y, z$; #5 $-x + 1, -y + 1, -z$; #6 $-x + {}^3/_2, y - ½, -z + {}^3/_2$; #7 $x, y, z - 1$; #8 $-x + 1, -y + 1, -z + 1$.

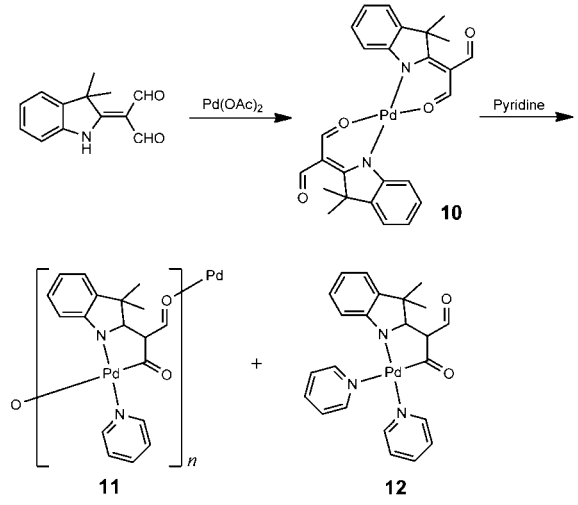

Scheme 4.

The ligand in these two complexes chelates the metal ion, not in the *N*,*O*-chelating mode observed in the former complexes, but in a *C*,*N*-chelating fashion. Interestingly, in the presence of pyridine, aldehyde C–H bond activation occurs at the Pd^{II} center, thus the dianionic diformyl compound binds to the metal center through its carbonyl carbon C10 and the nitrogen donor atom to form a five-membered metallocycle. This type of cyclometalation of aldehyde functions is not without precedent and has been reported in palladium(II) complexes of quinoline-8-carbaldehyde and dimethylamino-benzaldehyde.[26,27] Such organopalladium species have been utilized as intermediates in the double carbonylation of aromatic compounds to give α-keto amides.[28]

In complex **11**, the palladium ion is coordinated by the nitrogen and carbonyl C10 from one diformyl ligand and O2 of a symmetry-related diformyl ligand into polymeric linear chains along the *c* axis (Figure 7). Thus, the doubly deprotonated diformyl behaves as a *C*,*N*,*O*-tridentate chelating-bridging agent. One coordinated pyridine molecule completes a distorted square-planar environment around the palladium atom that is displaced 0.0398(9) Å out of the coordination plane (C10–N1–O2–N2). The distortion from the ideal square-planar geometry is also evident from the C10–Pd1–N1 bite angle of 80.95(8)° and N1–Pd1–N2 angle of 174.52(6)° (Table 5).

In contrast to the polymeric structure of **11**, the structure of complex **12** consists of discrete mononuclear units in which the doubly deprotonated diformyl ligand acts as a *C*,*N*-bidentate chelate. Both oxygen atoms of the ligand remain uncoordinated to the metal ion and are engaged in C–H···O hydrogen-bonding interactions (Table 6). The square-

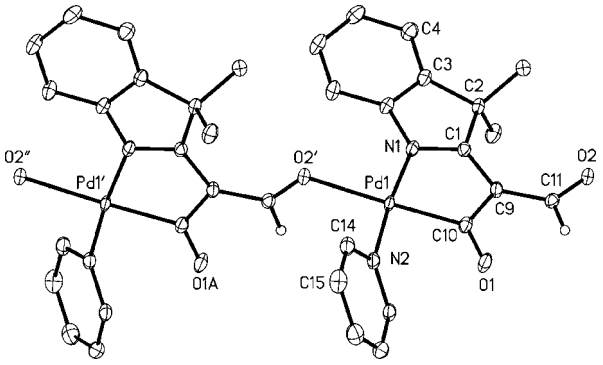

Figure 7. The crystal structure and atom-labeling scheme of coordination polymer **11** (50% probability ellipsoids). The hydrogen atoms, except for the aldehyde hydrogen atoms, have been omitted for clarity.

planar geometry around the palladium(II) atom is completed by two pyridine ligands, the dihedral angle between them being 83.57(13)°. The deviation from the ideal geometry is reflected by the disposition of the metal center 0.0069(12) Å out of the coordination plane and coordination bond angles of 80.88(2)–177.16(11)° (Table 5). The Pd–C10 bond length of 1.997(3) Å is typical for a Pd–acyl carbon distance, and the Pd–N distances lie in the normal range. The longer bond length of Pd1–N3 than that of Pd1–N2 points to the large *trans* influence associated with the acyl group, as has been observed in similar acyl–palladium(II) complexes.[29,30]

An interesting feature of the structure is the occurrence of a C–H···Pd interaction with Pd···H distance of 2.80(4) Å and Pd–H–C angle of 163(3)°, which connects two molecules into a centrosymmetric dimer (Figure 8). This interaction can best be regarded as an anagostic interaction that is characterized by an M···H distance of around 2.3–2.9 Å and an M–H–C bond angle of 110–170° and is typically associated with square-planar d^8 metal centers.[31] The nature of this type of interaction is still ambiguous and may involve donation of filled $d_{xz/yz}$ orbitals of the metal center into the C–H σ* orbital.[32]

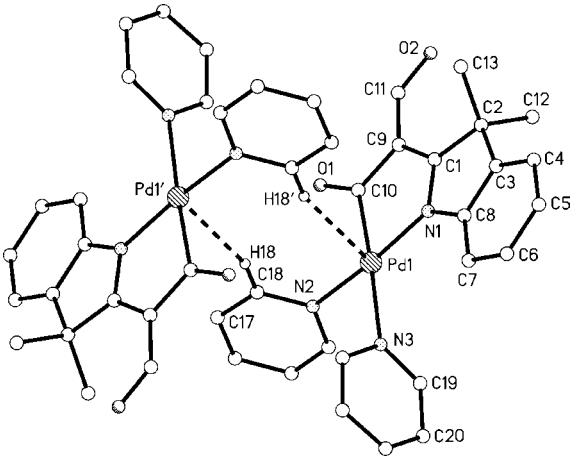

Figure 8. A perspective view of two molecules of **12** connected through Pd···H anagostic interactions.

From the formation of acyl–palladium(II) complexes **11** and **12**, one might expect that using 4,4′-bipyridine instead of pyridine in the reaction with the initial palladium complex, **10**, would lead to a bipyridine-bridged acyl–palladium complex. This presumption was confirmed by the crystal structure of **13**, obtained from a solution of **10** and 4,4′-bipyridine in DMF (Figure 9). In the structure, the Pd^{II} ion is four-coordinated by the dianionic diformyl ligand as a *C*,*N*-bidentate chelate and two bridging 4,4′-bipy ligands in a square-planar coordination environment.

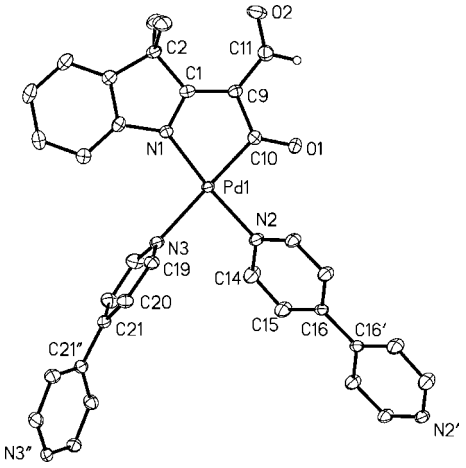

Figure 9. The crystal structures and atom-labeling schemes of **13**. The co-crystallized DMF molecule and also the hydrogen atoms, except for the aldehyde hydrogen atom, have been omitted for clarity.

The deviation from the ideal geometry is reflected in *cisoid* angles [80.95(8)–99.95(7)°] and *transoid* angles [178.88(8)° and 174.36(7)°] (Table 5), and also the disposition of the palladium(II) atom 0.0106(10) Å out of the coordination plane. Similar to what was observed in complex **12**, the large *trans* influence of the acyl group is evident from the longer bond length of Pd1–N3 [2.2205(19) Å] than

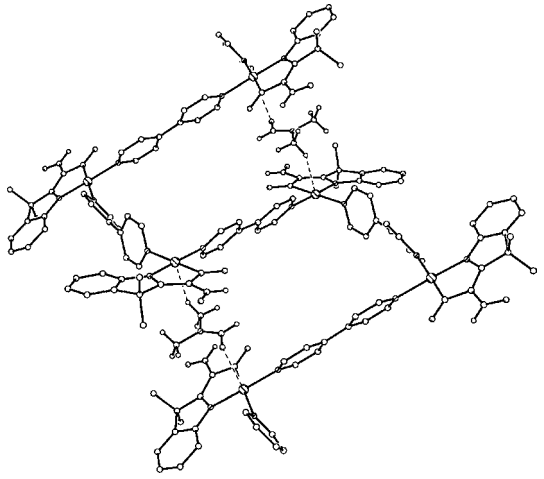

Figure 10. Infinite loop of coordination polymer **13**, showing Pd···O and anagostic Pd···H interactions with the co-crystallized DMF molecules.

that of Pd1–N2 [2.0955(19) Å]. The adjacent palladium centers are bridged by two conformationally different 4,4′-bipy ligands, one of which is planar, whereas the other one is significantly twisted [47.47(6)°] about the central C–C bond, thereby resulting in an infinite looped chain that runs along the *c* axis (Figure 10). The crystal structure consists of the coordination polymer and half of the disordered DMF solvent molecule per each palladium atom. The DMF molecules are sandwiched between the metal centers and stabilize the loop structure by a weak Pd···O interaction [Pd1···O5 3.370(4) Å] and a Pd···H interaction. Once again, the geometric parameters of the Pd···H interaction (Pd1···H26C 2.5828 Å; Pd1–H26C–C26 131.50°) suggest its anagostic nature.

Conclusion

2-(Diformylmethylene)-3,3-dimethylindole can react with the selected transition-metal ions to give the corresponding metal-organic compounds with a variety of structures. The structure of the complexes can be mononuclear, dinuclear, or polynuclear, depending on the bonding mode of the ambidentate ligand, the geometry adopted by the metal centers, and the presence and entity of ancillary ligands. Coordination environments vary from square-planar (Pd^{II}) to [4+1] distorted square-pyramidal (Cu^{II} and Pd^{II}) to octahedral (Co^{II}, Ni^{II}, Zn^{II} and Cd^{II}). In the resulting complexes, the diformyl ligand shows *N*,*O*-chelating or *N*,*O*,*O*-chelating-bridging modes when is monoanionic. Upon reaction with a pyridine-like ligand, the initial *N*,*O*-chelated palladium complex can undergo aldehyde C–H bond activation and gives the acyl–palladium complexes wherein the dianionic diformyl adopts *C*,*N*-chelating or *C*,*N*,*O*-chelating-bridging coordination fashion. Aside from the coordinating interactions, different noncovalent interactions (hydrogen-bonding and anagostic interactions) were observed to define the architecture of the structures.

Experimental Section

Materials and Measurements: 2,3,3-Trimethylindolenine was purchased from the Aldrich–Sigma Company. Ethanol was distilled prior to use. Magnetic susceptibilities were measured with a Sherwood Scientific MSB-AUTO magnetic susceptibility balance at 298 K. Diamagnetic corrections were applied using Pascal's constants. The IR spectra were taken with a Perkin–Elmer Spectrum 400 ATR-FTIR spectrometer. The NMR spectra were recorded with a JEOL Lambda 400 MHz FT-NMR spectrometer. The electronic spectra were measured with a Shimadzu UV-3600 UV/Vis/NIR spectrophotometer in the region of 200–1200 nm.

Synthesis of 2-(Diformylmethylene)-3,3-dimethylindole: The diformyl compound was prepared by the action of Vilsmeier reagent ($DMF/POCl_3$) on 2,3,3-trimethylindolenine as described previously.[8] IR (ATR): $\tilde{\nu}$ = 3146 (m), 2856 (w), 1661 (s), 1647 (s), 1629 (s), 1610 (s), 1509 (s), 1466 (s), 1218 (m), 1197 (m), 520 (m), 477 (m) cm^{-1}. ^1H NMR ($CDCl_3$): δ = 13.56 (s, 1 H, N*H*), 9.79 (s, 1 H, C*H*O), 9.77 (s, 1 H, C*H*O), 7.33–7.35 (m, 1 H, Ar–*H*), 7.31 (dd, 1 H, *J* = 7.6, 1.3 Hz, Ar–*H*), 7.25 (td, 1 H, *J* = 7.6, 1.3 Hz, Ar–*H*), 7.19 (d, 1 H, *J* = 7.6 Hz, Ar–*H*), 1.76 (s, 6 H, CH_3) ppm. ^{13}C NMR ($CDCl_3$): δ = 192.43, 187.85 (*C*HO), 179.45 (OCH*C*CHO), 140.70, 139.45, 128.35, 125.74, 122.23, 112.78, 109.52 (*Ar*), 51.36 (CH_3CCH_3), 23.55 (CH_3CCH_3) ppm.

Cobalt(II) Complexes 1 and 2: A mixture of diformyl (0.43 g, 2.0 mmol) and cobalt(II) acetate tetrahydrate (0.25 g, 1.0 mmol) in ethanol (10 mL) along with a few drops of triethylamine was heated at reflux for 1 h and then cooled to room temperature. The resulting orange precipitate, $[Co(C_{13}H_{12}NO_2)_2(H_2O)]$ (**1**), was filtered off, washed with ethanol, and dried with silica gel; yield 0.295 g, 58%. $C_{26}H_{26}CoN_2O_5$ (505.44): calcd. C 61.78, H 5.18, N 5.54; found C 61.75, H 4.88, N 5.44. IR (ATR): $\tilde{\nu}$ = 3553 (w), 2822 (vw), 2782 (vw), 1635 (m), 1542 (vs), 1455 (s), 1201 (m), 503 (m), 480 (m) cm^{-1}. UV/Vis (solid): λ_{max} = 1080, 389, 271 nm. μ_{eff} = 5.41 B.M.

A solution of complex **1** in a mixture of chloroform and pyridine yielded orange crystals of $[Co(C_{13}H_{12}NO_2)_2(py)_2]$ (**2**) after one week. $C_{36}H_{34}CoN_4O_4$ (645.62): calcd. C 66.97, H 5.31, N 8.68; found C 66.48, H 5.09, N 8.38. IR (ATR): $\tilde{\nu}$ = 2748 (vw), 2720 (vw), 1655 (m), 1550 (vs), 1441 (s), 1193 (m), 499 (m), 468 (m), 428 (w) cm^{-1}. UV/Vis (solid): λ_{max} = 1017, 744, 635, 384, 268, 233 nm. μ_{eff} = 4.91 B.M.

Nickel(II) Complexes 3 and 4: A mixture of diformyl (0.43 g, 2.0 mmol) and nickel(II) acetate tetrahydrate (0.25 g, 1.0 mmol) along with a few drops of triethylamine in ethanol (10 mL) was heated at reflux for 1 h and then left at room temperature overnight. The resulting green precipitate, $[Ni(C_{13}H_{12}NO_2)_2(H_2O)_2]$ (**3**), was filtered off, washed with aqueous ethanol (50%), and dried with silica gel; yield 0.283 g, 54%. $C_{26}H_{28}N_2NiO_6$ (523.23): calcd. C 59.69, H 5.39, N 5.35; found C 59.83, H 4.97, N 5.40. IR (ATR): $\tilde{\nu}$ = 3384 (br), 2862 (vw), 1622 (m), 1544 (vs), 1452 (s), 1206 (m), 499 (m), 480 (w) cm^{-1}. UV/Vis (solid): λ_{max} = 1023, 614, 395, 278, 223 nm. μ_{eff} = 2.97 B.M.

Slow evaporation of a solution of the complex **3** in a mixture of DMF and pyridine afforded dark green crystals of $[Ni(C_{13}H_{12}NO_2)_2(py)_2]$ (**4**). $C_{36}H_{34}N_4NiO_4$ (645.40): calcd. C 67.00, H 5.31, N 8.68; found C 67.39, H 5.12, N 8.73. IR (ATR): $\tilde{\nu}$ = 2778 (vw), 2720 (w), 1664 (m), 1559 (vs), 1440 (s), 1194 (m), 500 (m), 471 (m), 434 (m) cm^{-1}. UV/Vis (solid): λ_{max} = 974, 712, 566, 334, 264 nm. μ_{eff} = 3.15 B.M.

Copper(II) Complex 5: A solution of copper(II) acetate monohydrate (0.2 g, 1.0 mmol) in ethanol (30 mL) was added to an ethanolic solution (30 mL) of diformyl (0.43 g, 2.0 mmol) followed by addition of a few drops of triethylamine. The mixture was heated at reflux for 15 min and then cooled to room temperature. The resulting green precipitate, $[Cu(C_{13}H_{12}NO_2)_2]_2$ (**5**), was washed with ethanol and dried with silica gel; yield 0.464 g, 94%. $C_{26}H_{24}CuN_2O_4$ (492.03): calcd. C 63.47, H 4.92, N 5.69; found C 63.48, H 4.79, N 5.63. IR (ATR): $\tilde{\nu}$ = 2733 (w), 1673 (m), 1658 (m), 1552 (vs), 1438 (s), 1194 (m), 503 (m), 495 (m), 480 (m), 418 (m) cm^{-1}. UV/Vis (solid): λ_{max} = 637, 384, 290, 231 nm. μ_{eff} = 1.96 B.M.

The X-ray quality crystal of **5** was obtained from a dimethyl sulfoxide (DMSO) solution at room temperature.

Zinc(II) Complexes 6 and 7: An ethanolic solution (10 mL) of diformyl (0.43 g, 2.0 mmol) and zinc(II) acetate dihydrate (0.22 g, 1.0 mmol) in the presence of a few drops of triethylamine was heated at reflux for 1 h and then cooled to room temperature. Water (1 mL) was added, and the resulting white precipitate was collected, washed with water, and recrystallized from ethanol to give the colorless crystals of $[Zn(C_{13}H_{12}NO_2)_2]_n$ (**6**); yield 0.217 g,

44%. $C_{26}H_{24}N_2O_4Zn$ (493.87): calcd. C 63.23, H 4.90, N 5.67; found C 63.18, H 4.66, N 5.41. IR (ATR): $\tilde{\nu}$ = 2814 (w), 2778 (w), 1639 (m), 1556 (vs), 1456 (s), 1205 (s), 502 (m), 478 (m) cm^{-1}.

Recrystallization of **6** from methanol afforded the colorless crystals of $[Zn(C_{13}H_{12}NO_2)_2(CH_4O)_2]$ (**7**). $C_{28}H_{32}N_2O_6Zn$ (557.95): calcd. C 60.27, H 5.78, N 5.02; found C 59.99, H 5.43, N 5.11. IR (ATR): $\tilde{\nu}$ = 2700–3400 (br), 1637 (m), 1549 (vs), 1445 (s), 1195 (m), 1034 (s), 498 (m), 466 (m) cm^{-1}.

Cadmium(II) Complexes 8 and 9: An ethanolic solution (10 mL) of diformyl (0.43 g, 2.0 mmol) and cadmium(II) acetate dihydrate (0.27 g, 1 mmol) along with a few drops of triethylamine was heated at reflux for 1 h and then left at room temperature for a few hours, whereupon the colorless crystals of $[Cd(C_{13}H_{12}NO_2)_2]_n$ (**8**) were obtained; yield 0.314 g, 58%. $C_{26}H_{24}CdN_2O_4$ (540.89): calcd. C 57.73, H 4.47, N 5.18; found C 57.44, H 4.89, N 5.32. IR (ATR): $\tilde{\nu}$ = 2818 (w), 2774 (w), 1638 (m), 1559 (vs), 1456 (s), 1204 (s), 498 (m), 472 (m) cm^{-1}.

Recrystallization of **8** from methanol led to the formation of $[Cd(C_{13}H_{12}NO_2)_2(CH_4O)_2]$ (**9**) as colorless crystals. $C_{28}H_{32}CdN_2O_6$ (604.97): calcd. C 55.59, H 5.33, N 4.63; found C 55.42, H 5.03, N 4.61. IR (ATR): $\tilde{\nu}$ = 2700–3400 (br), 1633 (m), 1545 (vs), 1445 (s), 1196 (m), 1033 (s), 495 (m), 465 (m) cm^{-1}.

Palladium(II) Complexes 10, 11, 12, and 13: A solution of palladium(II) acetate (0.23 g, 1.0 mmol) in ethanol (20 mL) was added to an ethanolic solution (10 mL) of diformyl (0.43 g, 2.0 mmol) followed by addition of a few drops of triethylamine. The mixture was heated at reflux for 15 min and then cooled to room temperature. The precipitate, $[Pd(C_{13}H_{12}NO_2)_2]$ (**10**), was filtered off, washed with ethanol, and dried with silica gel; yield 0.473 g, 88%. $C_{26}H_{24}N_2O_4Pd$ (534.89): calcd. C 58.38, H 4.52, N 5.24; found C 58.11, H 4.58, N 5.52. IR (ATR): $\tilde{\nu}$ = 2743 (w), 2717 (w), 1674 (s), 1539 (vs), 1436 (s), 1189 (m), 508 (m), 493 (m), 439 (w) cm^{-1}. UV/Vis (solid): λ_{max} = 382, 321, 234 nm. ^1H NMR ($CDCl_3$): δ = 9.54 (s, 1 H, C*H*O), 7.86 (d, 1 H, J = 7.2 Hz, Ar–*H*), 7.73 (s, 1 H, C*H*O), 7.27–7.32 (m, 3 H, Ar–*H*), 1.66 (s, 6 H, CH_3) ppm. ^{13}C NMR ($CDCl_3$): δ = 188.91 (*C*HO), 185.27 (*C*HO), 178.19 (OCH*C*CHO), 147.23, 145.43, 127.42, 126.26, 121.14, 119.41, 116.76 (*Ar*), 52.57 (CH_3CCH_3), 23.01 (CH_3) ppm.

X-ray quality single crystals of **10** were obtained by slow evaporation of a dioxane solution at room temperature. Recrystallization of **10** from a mixture of DMF and pyridine at room temperature yielded the crystals of $[Pd(C_{13}H_{11}NO_2)(py)]_n$ (**11**) and $[Pd(C_{13}H_{11}NO_2)(py)_2]$ (**12**). Using 4,4′-bipyridine instead of pyridine led to the formation of $\{[Pd(C_{13}H_{11}NO_2)(bipy)]\cdot 0.5DMF\}_n$ (**13**).

Crystallography: Diffraction data were measured with a Bruker SMART Apex II CCD area-detector diffractometer (graphite-monochromated Mo-K_α radiation, λ = 0.71073 Å). The orientation matrix, unit-cell refinement, and data reduction were all handled by the Apex2 software (SAINT integration, SADABS absorption correction.[33]) The structures were solved using direct or Patterson methods in the program SHELXS-97 and were refined by the full-matrix least-squares method on F^2 with SHELXL-97.[34] All the non-hydrogen atoms were refined anisotropically and all the C-bound hydrogen atoms were placed at calculated positions and refined isotropically. O-bound hydrogen atoms were located in difference Fourier maps and refined with distance restraint of O–H 0.84(2) Å. Drawings of the molecules were produced with XP.[34] Crystal data and refinement are summarized in Tables 7, 8, and 9.

Table 7. Crystal data and refinement parameters for the cobalt(II), nickel(II), and copper(II) complexes.

	$[Co(C_{13}H_{12}NO_2)_2(py)_2]$ (**2**)	$[Ni(C_{13}H_{12}NO_2)_2(py)_2]$ (**4**)	$[Cu(C_{13}H_{12}NO_2)_2]_2$ (**5**)
Empirical formula	$C_{36}H_{34}CoN_4O_4$	$C_{36}H_{34}N_4NiO_4$	$C_{52}H_{48}Cu_2N_4O_8$
M_r	645.60	645.38	984.02
T [K]	103(2)	296(2)	100(2)
Crystal system	triclinic	triclinic	monoclinic
Space group	$P\bar{1}$	$P\bar{1}$	$P21/c$
a [Å]	11.1749(10)	10.8259(7)	7.0057(14)
b [Å]	12.3090(11)	12.3814(9)	26.565(5)
c [Å]	13.7367(12)	13.8481(9)	11.849(2)
α [°]	81.537(2)	83.782(4)	–
β [°]	71.2310(10)	81.876(4)	96.912(4)
γ [°]	64.2050(10)	64.616(4)	–
V [Å^3]	1610.7(2)	1657.80(19)	2189.0(7)
Z	2	2	2
$\rho_{calcd.}$ [g cm^{-3}]	1.331	1.294	1.493
Absorption coefficient [mm^{-1}]	0.578	0.629	1.035
F(000)	674	676	1020
Crystal size [mm^3]	0.41 × 0.31 × 0.05	0.60 × 0.20 × 0.13	0.30 × 0.13 × 0.05
θ range for data collection [°]	1.57 to 25.00	1.49 to 25.00	1.53 to 25.00
Index ranges	$-13 \le h \le 12$, $-14 \le k \le 14$, $-16 \le l \le 12$	$-12 \le h \le 12$, $-14 \le k \le 14$, $-16 \le l \le 16$	$-8 \le h \le 7$, $-31 \le k \le 31$, $-12 \le l \le 14$
Reflections collected/unique	7623/5536 [R_{int} = 0.0200]	9403/5735 [R_{int} = 0.0734]	10109/3844 [R_{int} = 0.0705]
Completeness to θ = 25.00° [%]	97.4	98.1	99.6
Max./min. transmission	0.975/0.798	0.923/0.704	0.950/0.747
Data/restraints/parameters	5536/1/410	5735/2/410	3844/12/302
Goodness-of-fit on F^2	1.048	0.932	1.008
Final R indices [$I > 2\sigma(I)$]	R_1 = 0.0377, wR_2 = 0.0975	R_1 = 0.0537, wR_2 = 0.1213	R_1 = 0.0492, wR_2 = 0.1027
R indices (all data)	R_1 = 0.0503, wR_2 = 0.1120	R_1 = 0.0997, wR_2 = 0.1390	R_1 = 0.0926, wR_2 = 0.1167
Largest diff. peak/hole [e Å^{-3}]	0.313/–0.272	0.916/–0.365	0.378/–0.517

Table 8. Crystal data and refinement parameters for the zinc(II) and cadmium(II) complexes.

	$[Zn(C_{13}H_{12}NO_2)_2]_n$ (**6**)	$[Zn(C_{13}H_{12}NO_2)_2(CH_4O)_2]$ (**7**)	$[Cd(C_{13}H_{12}NO_2)_2]_n$ (**8**)	$[Cd(C_{13}H_{12}NO_2)_2(CH_4O)_2]$ (**9**)
Empirical formula	$C_{26}H_{24}N_2O_4Zn$	$C_{28}H_{32}N_2O_6Zn$	$C_{26}H_{24}CdN_2O_4$	$C_{28}H_{32}CdN_2O_6$
M_r	493.84	557.93	540.87	604.96
T [K]	296(2)	113(2)	100(2)	100(2)
Crystal system	rhombohedral	monoclinic	rhombohedral	monoclinic
Space group	$R\bar{3}:r$	$P21/c$	$R\bar{3}:r$	$P21/c$
a [Å]	12.6074(3)	11.402(6)	12.8387(7)	11.5456(2)
b [Å]	12.6074(3)	9.447(5)	12.8387(7)	9.62180(10)
c [Å]	12.6074(3)	12.139(6)	12.8387(7)	11.9139(2)
α [°]	104.04	–	103.93	–
β [°]	104.04	94.409(9)	103.93	93.8480(10)
γ [°]	104.04	–	103.93	–
V [Å^3]	1786.60(7)	1303.6(11)	1890.73(18)	1320.53(3)
Z	3	2	3	2
$\rho_{calcd.}$ [g cm^{-3}]	1.377	1.421	1.425	1.521
Absorption coefficient [mm^{-1}]	1.065	0.987	0.899	0.872
F(000)	768	584	822	620
Crystal size [mm^3]	0.45 × 0.35 × 0.13	0.60 × 0.50 × 0.08	0.36 × 0.27 × 0.20	0.39 × 0.29 × 0.07
θ range for data collection [°]	1.76 to 27.49	1.79 to 25.25	1.72 to 26.99	2.72 to 27.50
Index ranges	$-16 \le h \le 13$, $-16 \le k \le 15$, $-16 \le l \le 15$	$-13 \le h \le 13$, $-9 \le k \le 11$, $-14 \le l \le 14$	$-16 \le h \le 16$, $-16 \le k \le 16$, $-12 \le l \le 16$	$-14 \le h \le 15$, $-12 \le k \le 12$, $-15 \le l \le 15$
Reflections collected/unique	10357/2743 [R_{int} = 0.0297]	5976/2354 [R_{int} = 0.0186]	2763 [R_{int} = 0.0463]	9378/3038 [R_{int} = 0.0216]
Completeness	to θ = 27.49°: 100.0%	to θ = 25.00°: 99.7%	to θ = 26.99°: 100.0%	to θ = 26.00°: 99.9%
Max./min. transmission	0.874/0.646	0.925/0.589	0.841/0.738	0.942/0.727
Data/restraints/parameters	2743/6/153	2354/1/175	2763/0/153	3038/8/175
Goodness-of-fit on F^2	1.027	1.075	1.048	1.049
Final R indices [$I > 2\sigma(I)$]	R_1 = 0.0289, wR_2 = 0.0704	R_1 = 0.0241, wR_2 = 0.0635	R_1 = 0.0247, wR_2 = 0.0487	R_1 = 0.0212, wR_2 = 0.0499
R indices (all data)	R_1 = 0.0389, wR_2 = 0.0748	R_1 = 0.0277, wR_2 = 0.0659	R_1 = 0.0293, wR_2 = 0.0503	R_1 = 0.0266, wR_2 = 0.0520
Largest diff. peak/hole [e Å^{-3}]	0.304/–0.243	0.297/–0.237	0.393/–0.336	0.337/–0.533

Table 9. Crystal data and refinement parameters for the palladium(II) complexes.

	$[Pd(C_{13}H_{12}NO_2)_2]$ (**10**)	$[Pd(C_{13}H_{11}NO_2)(py)]_n$ (**11**)	$[Pd(C_{13}H_{11}NO_2)(py)_2]$ (**12**)	$\{[Pd(C_{13}H_{11}NO_2)(bipy)]\cdot 0.5DMF\}_n$ (**13**)
Empirical formula	$C_{26}H_{24}N_2O_4Pd$	$C_{18}H_{16}N_2O_2Pd$	$C_{23}H_{21}N_3O_2Pd$	$C_{49}H_{45}N_7O_5Pd_2$
M_r	534.87	398.73	477.83	1024.72
T [K]	100(2)	100(2)	296(2)	100(2)
Crystal system	monoclinic	monoclinic	monoclinic	monoclinic
Space group	$P21/c$	$P21/c$	$P21/n$	$C2/c$
a [Å]	7.0992(3)	6.5234(3)	9.58720(10)	15.4998(2)
b [Å]	26.6053(12)	17.4032(9)	17.4169(2)	17.2185(2)
c [Å]	11.6933(5)	14.0460(7)	12.6524(2)	16.5477(2)
β [°]	95.359(3)	91.6560(10)	93.0040(10)	93.954(2)
V [Å^3]	2198.93(17)	1593.95(14)	2109.79(5)	4405.79(9)
Z	4	4	4	4
$\rho_{calcd.}$ [g cm^{-3}]	1.616	1.662	1.504	1.545
Absorption coefficient [mm^{-1}]	0.881	1.175	0.903	0.873
F(000)	1088	800	968	2080
Crystal size [mm^3]	0.28 × 0.05 × 0.02	0.32 × 0.19 × 0.04	0.25 × 0.17 × 0.09 mm	0.33 × 0.25 × 0.20 mm
θ range for data collection [°]	2.32 to 25.04	2.34 to 27.00	1.99 to 25.25	2.11 to 25.50
Index ranges	$-8 \le h \le 8$, $-31 \le k \le 31$, $-13 \le l \le 13$	$-8 \le h \le 8$, $-22 \le k \le 22$, $-17 \le l \le 17$	$-11 \le h \le 11$, $-20 \le k \le 20$, $-15 \le l \le 15$	$-18 \le h \le 18$, $-20 \le k \le 20$, $-20 \le l \le 20$
Reflections collected/unique	15577/3885 [R_{int} = 0.1318]	19265/3481 [R_{int} = 0.0337]	12337/3820 [R_{int} = 0.0199]	17779/4088 [R_{int} = 0.0299]
Completeness	to θ = 25.00°: 99.7%	to θ = 27.00°: 99.9%	to θ = 25.00°: 99.9%	to θ = 25.00°: 100.0%
Max./min. transmission	0.983/0.791	0.955/0.705	0.927/0.806	0.845/0.762
Data/restraints/parameters	3885/18/302	3481/0/210	3820/2/264	4088/0/275
Goodness-of-fit on F^2	1.182	1.040	1.057	1.039
Final R indices [$I > 2\sigma(I)$]	R_1 = 0.0794, wR_2 = 0.1627	R_1 = 0.0214, wR_2 = 0.0487	R_1 = 0.0328, wR_2 = 0.0925	R_1 = 0.0246, wR_2 = 0.0572
R indices (all data)	R_1 = 0.1270, wR_2 = 0.1763	R_1 = 0.0254, wR_2 = 0.0505	R_1 = 0.0381, wR_2 = 0.0968	R_1 = 0.0282, wR_2 = 0.0593
Largest diff. peak/hole [e Å^{-3}]	1.694/–1.350	0.432/–0.405	1.573/–0.504	0.771/–0.515

CCDC-805122 (for **2**), -805123 (for **4**), -805124 (for **5**), -805125 (for **6**), -805126 (for **7**), -805127 (for **8**), -805128 (for **9**), -805118 (for **10**), -805119 (for **11**), -805120 (for **12**), and -805121 (for **13**) contain the supplementary crystallographic data for this paper. These data can be obtained free of charge from The Cambridge Crystallographic Data Centre via www.ccdc.cam.ac.uk/data_request/cif.

Acknowledgments

Financial support from the University of Malaya is highly appreciated (FRGS grant number FP004/2010B).

[1] Z. He, C. He, Z.-M. Wang, E.-Q. Gao, Y. Liu, C.-H. Yan, *Dalton Trans.* **2004**, 502–504.
[2] D. A. Beauchamp, S. J. Loeb, *Chem. Commun.* **2002**, 2484–2485.
[3] J. E. Beves, B. E. Chapman, P. W. Kuchel, L. F. Lindoy, J. McMurtrie, M. McPartlin, P. Thordarson, G. Wei, *Dalton Trans.* **2006**, 744–750.
[4] L. Carlucci, G. Ciani, D. M. Proserpio, *Chem. Commun.* **2004**, 380–381.
[5] X.-H. Bu, W. Chen, S.-L. Lu, R.-H. Zhang, D.-Z. Liao, W.-M. Bu, M. Shionoya, F. Brisse, J. Ribas, *Angew. Chem.* **2001**, *113*, 3301; *Angew. Chem. Int. Ed.* **2001**, *40*, 3201–3203.
[6] X. Li, R. Cao, Z. Guo, Y. Wang, X. Zhu, *J. Mol. Struct.* **2006**, *798*, 64–68.
[7] M. Helliwell, A. Afgan, M. M. Baradarani, J. A. Joule, *Acta Crystallogr., Sect. E* **2006**, *62*, o737.
[8] H. Khaledi, S. M. Saharin, H. M. Ali, W. T. Robinson, M. A. Abdulla, *Acta Crystallogr., Sect. E* **2009**, *65*, o2585.K.
[9] Neuvonen, C. Zewi, H. Lönnberg, *Acta Chem. Scand.* **1996**, *50*, 1137–1142.
[10] B. Chiari, A. Cinti, O. Crispu, F. Demartin, A. Pasini, O. Piovesana, *J. Chem. Soc., Dalton Trans.* **2001**, 3611–3616.
[11] H. Tamura, K. Ogawa, R. Ryu, M. Tanaka, T. Shono, I. Masuda, *Inorg. Chim. Acta* **1981**, *50*, 101–109.
[12] U. Casellato, P. Guerriero, S. Tamburini, P. A. Vigato, R. Graziani, *Inorg. Chim. Acta* **1986**, *119*, 75–82.
[13] D. Pucci, A. Bellusci, A. Crispini, M. Ghedini, M. La Deda, *Inorg. Chim. Acta* **2004**, *357*, 495–504.
[14] A. W. Addison, T. N. Rao, J. Reedijk, V. J. Rijn, G. C. Verschoor, *J. Chem. Soc., Dalton Trans.* **1984**, 1349–1356.
[15] D.-C. Wen, S.-X. Liu, J. Ribas, *Inorg. Chem. Commun.* **2007**, *10*, 661–665.
[16] A. L. Spek, *PLATON*, Utrecht University, Utrecht, The Netherlands, **2010**.
[17] R. W. Saalfrank, R. Harbig, O. Struck, E.-M. Peters, K. Peters, H. G. von Schnering, *Z. Naturforsch. B: J. Chem. Sci.* **1996**, *51*, 399–408.
[18] X.-Y. Qiu, *Acta Crystallogr., Sect. E* **2006**, *62*, m1091.
[19] Y.-N. Liu, G. Orlowski, G. Schatte, H.-B. Kraatz, *Inorg. Chim. Acta* **2005**, *358*, 1151–1161.
[20] H. Iida, Y. Yuasa, C. Kibayashi, Y. Iitaka, *J. Chem. Soc., Dalton Trans.* **1981**, 2212–2216.
[21] A. J. Canty, N. J. Minchin, L. M. Engelhardt, B. W. Skelton, A. H. White, *Aust. J. Chem.* **1988**, *41*, 651–665.
[22] M. Mikuriya, K. Minowa, J.-W. Lim, *Bull. Chem. Soc. Jpn.* **2001**, *74*, 331–332.
[23] S. M. O. Quintal, H. I. S. Nogueira, V. Felix, M. G. B. Drew, *New J. Chem.* **2000**, *24*, 511–517.
[24] J.-F. Ma, Y. Kojima, Y. Yamamoto, *J. Organomet. Chem.* **2000**, *616*, 149–156.
[25] M. H. Johansson, A. Oskarsson, *Acta Crystallogr., Sect. C* **2001**, *57*, 1265–1267.
[26] C. G. Anklin, P. S. Pregosin, *J. Organomet. Chem.* **1983**, *243*, 101–109.
[27] A. Albinati, C. G. Anklin, F. Ganazzoli, H. Ruegg, P. S. Pregosin, *Inorg. Chem.* **1987**, *26*, 503–508.
[28] F. Ozawa, I. Yamagami, M. Nakano, *Chem. Lett.* **1989**, 125–128.
[29] J. Vicente, J.-A. Abad, A. D. Frankland, M. C. Ramirez de Arellano, *Chem. Eur. J.* **1999**, *5*, 3066–3075.
[30] F. Paul, J. Fischer, P. Ochsenbein, J. A. Osborn, *Angew. Chem.* **1993**, *105*, 1687; *Angew. Chem. Int. Ed. Engl.* **1993**, *32*, 1638–1640.
[31] M. Brookhart, M. L. H. Green, G. Parkin, *Proc. Natl. Acad. Sci. USA* **2007**, *104*, 6909–6914.
[32] Y. Zhang, J. C. Lewis, R. G. Bergman, J. A. Ellman, E. Oldfield, *Organometallics* **2006**, *25*, 3515–3519.
[33] *Bruker APEX2, SAINT* and *SADABS*, Bruker AXS Inc., Madison, WI, USA, **2007**.
[34] G. M. Sheldrick, *Acta Crystallogr., Sect. A* **2008**, *64*, 112–122.
Received: January 16, 2011
Published Online: April 7, 2011

